*Rev. Soc. Quím. Méx.* **2004**, *48, 260-268*

*Investigación*

# Synthesis and Characterization of Simultaneously-Impregnated Co-Mo-P on Al-MCM41. Effect of Support Precursors

Agileo Hernández,[1] José Escobar,*, [1] José G. Pacheco,[2] José A. de los Reyes,[3] and María C. Barrera[3]

[1] Instituto Mexicano del Petróleo, Eje Central Lázaro Cárdenas 152, San Bartolo Atepehuacan, Gustavo A. Madero, México, D.F. 07730, Tel.: (55) 91758389, Fax: (55) 91758429, E-mail: jeaguila@imp.mx
[2] División Académica de Ciencias Básicas, Universidad Juárez Autónoma de Tabasco, Km. 1, Carretera Cunduacán-Jalpa de Méndez, Cunduacán, Tabasco
[3] Área de Ingeniería Química, UAM-Iztapalapa, Av. San Rafael Atlixco 186, Col. Vicentina, Iztapalapa, México, D. F., 09340

Recibido el 27 de junio del 2004; aceptado el 11 de noviembre del 2004

**Abstract.** Al-MCM-41 ($SiO_2/Al_2O_3$=200) materials from various Al and Si sources were synthesized. The calcined solids (823 K) were characterized by $N_2$ physisorption, X-ray diffraction and surface acidity measurements. The sample from tetraethyl orthosilicate-$Al(SO_4)_3$ had decreased surface area (836 $m^2/g$) and pore volume (0.88 $cm^3/g$), meanwhile the lowest amount of $Al^{3+}$ incorporated into the MCM41 walls was registered when $SiO_2$-boehmite was used as precursor. Co, Mo and P (~3, ~12.5 and ~1.6 weight %, respectively) were simultaneously impregnated on Al-MCM41. Surface acidity was notably increased after impregnation, probably by the contribution of $PO_4^{3-}$ groups deposited. After sulfiding ($H_2S/H_2$, 673 K), the oxidic impregnated precursor having both the best texture and the highest proportion of octahedral $Mo^{6+}$ (the one supported on Al-MCM41 from $SiO_2$-$Al(SO_4)_3$) was ~30% more active in dibenzothiophene hydrodesulfurization (HDS) than an $Al_2O_3$-supported commercial formulation of similar Co-Mo-P loading. For the Al-MCM41-supported catalyst, the high HDS activity and predominant selectivity to biphenyl suggested good Mo promotion by Co.
**Key words:** Al-MCM41, hydrothermal synthesis, CoMo catalyst, dibenzothiophene hydrodesulfurization

**Resumen.** Se sintetizaron materiales Al-MCM-41 ($SiO_2/Al_2O_3$=200) a partir de distintas fuentes de Al y Si. Los sólidos calcinados (823 K) se caracterizaron por fisisorción de $N_2$, difracción de rayos X y mediciones de acidez superficial. La muestra preparada a partir de tetraetil ortosilicato-$Al(SO_4)_3$ presentó área específica y volumen de poro menores (836 $m^2/g$ y 0.88 $cm^3/g$, respectivamente) mientras que la menor incorporación de $Al^{3+}$ a las paredes de los materiales MCM41 se registró cuando se utilizaron $SiO_2$ y boemita como precursores. Se impregnó simultáneamente Co, Mo y P (~3, ~12.5 y ~1.6 % en peso) sobre Al-MCM41. La acidez superficial se incrementó notablemente después de la impregnación debido probablemente a la contribución de grupos $PO_4^{3-}$ depositados. Después de la sulfuración ($H_2S/H_2$, 673 K), el precursor con mejor textura y con la mayor proporción de $Mo^{6+}$ octaédrico (el soportado sobre Al-MCM41 obtenido a partir de $SiO_2$-$Al(SO_4)_3$) fue ~30 % más activo en la hidrodesulfuración (HDS) de dibenzotiofeno que una formulación comercial con soporte de $Al_2O_3$ y contenido similar de fase Co-Mo-P. La alta actividad en HDS y selectividad altamente orientada hacia la obtención de bifenil sugirieron buena promoción del Mo por el Co en el catalizador soportado sobre Al-MCM41.
**Palabras clave:** Al-MCM41, síntesis hidrotérmica, catalizador CoMo, hidrodesulfuración de dibenzotiofeno.

## Introduction

To comply with very strict environmental regulations regarding sulfur content in oil-derived middle distillates that will be enabled in the near future, there is a need for improved hydrotreatment (HDT) catalysts that could eliminate the most refractory organo-sulfur compounds (*i.e.*, dibenzothiophenes with alkyl groups in the positions 4 and/or 6 of the aromatic rings). These species account for most of the S remaining (~300 ppm in weight) in straight-run gas oils hydrotreated under conventional conditions. Thus, to obtain cleaner fuels (ultra-low sulfur diesel of 15-50 ppm in weight S), development of more active hydrodesulfurization (HDS) catalysts is indispensable.

Substitution of traditional $CoMo/Al_2O_3$ catalysts by novel improved formulations has demanded extensive studies on new active phases [1] or modification of textural, structural or chemical properties of catalyst supports [2, 3]. In this context, MCM41 mesoporous sieves have attracted attention mainly owing to their high surface area that could, in theory, efficiently disperse high amounts of Co-Mo sulfides [4]. Also, their pore size distribution could be tuned to specific applications, depending on the feedstock to be treated. For instance, by using mesitylene, materials with pores wide enough to avoid diffusional limitations during HDT of middle distillates could be prepared [5]. In addition, the high pore volume that characterize MCM-41 solids could be advantageous during impregnation considering that the use of less concentrated solutions could be reflected in more dispersed supported phases.

Aluminum incorporation to MCM41 matrices have been widely used to impart acidic properties [6] that could be very convenient in HDT processes. Increased Lewis acidity could promote active phases dispersion [7] meanwhile protonic sites could isomerize sterically-hindered species as 4,6-

dimethyldibenzothiophene to more favorable configurations that could facilitate their hydrodesulfurization (HDS) (i. e., 2,8- or 3,7-dimetyl dibenzothiophene) [8]. However, surface acidity should be carefully modulated considering that strong sites could provoke undesirable cracking reactions that would result in decreased liquid yield. Also, those sites would accelerate catalysts deactivation by coke lay-down.

The effect of $SiO_2/Al_2O_3$ ratio of Al-MCM materials [9], Co-Mo loading [4,10] and type of feedstock [4,11,12], among other parameters, on the performance of the corresponding catalyst in the HDS of oil-derived feedstocks has been previously reported. However, to the best of our knowledge, the influence of using various Si and Al precursors on the suitability of these materials as HDS catalyst supports has not been addressed yet.

In this work, we report the effect of using different Si and Al precursors at a given $SiO_2/Al_2O_3$ ratio, on the characteristics of Al-MCM41 as Co-Mo-P catalyst supports. The materials were characterized by $N_2$ physisorption, low-angle XRD and acidity measurements (pyridine FTIR). Impregnated materials were studied by the same techniques to get insight into the changes produced by Co-Mo-P deposition. Also, coordination of impregnated $Mo^{6+}$ species were analyzed by UV-vis DRS. The impregnated precursor of both the best texture and the highest proportion of octahedral $Mo^{6+}$ was sulfided previously to be tested in the liquid-phase dibenzothiophene (DBT) HDS in a batch reactor under conditions close to those used in industrial facilities for the HDT of middle distillates (5.6 MPa, 593 K). Superior hydrodesulfurization activity, as to that of an $Al_2O_3$-supported commercial formulation of similar Co-Mo-P loading, was observed.

## Experimental

### Materials Synthesis

*Supports.* Al-MCM-41 mesoporous sieves were synthesized from $SiO_2$ + $Al_2(SO_4)_3.nH_2O$ ($14 < n < 18$), tetraethyl orthosilicate (TEOS) + $Al_2(SO_4)_3.nH_2O$ ($14 < n < 18$) or $SiO_2$ + $AlO(OH)_2$. Silicon oxide and aluminum sulfate were from Baker (both ~100 wt % purity). TEOS was from Aldrich (99 wt %) and boehmite was Catapal B (from Sasol, Germany). Hexadecyltrimethylammonium bromide (templating agent, 99 wt % from Aldrich) dissolved in water was mixed with a tetramethylammonium hydroxide (Aldrich, 97 wt %) aqueous solution containing the Si source. Then, the amount of Al source necessary to reach a $SiO_2/Al_2O_3$ = 200 (mol ratio) in the final material was added. The mixture was aged in an autoclave (Parr 4842) at 423 K (48 h, no stirring). After filtration, the recovered product was $H_2O$-washed until foam elimination (approximately 5 times) then dried at room temperature to total liquid evaporation. Calcining was carried out at 823 K under $N_2$ flow (Praxair). After 1 h at those conditions, the sample was allowed to cool down until room temperature. Finally, the gas flow was switched to air (Praxair, extra-dry degree) and the materials were annealed for 6 h. In both steps the heating ramp was 2 K/min while the gas flow was 4 L/h.

*Catalysts precursors.* A preparation method commonly applied for HDS catalysts manufacturing at commercial scale was used. Co, Mo and P (3.0, 12.5 and 1.6 wt %, nominal contents) were impregnated simultaneously on supports previously dried (2 h) at 373 K at incipient wetness through an aqueous solution of $Co(CH_3CO_2)_2.4H_2O$ (99.9 wt %) and $MoO_3$ (99.5 wt %, both from Baker). The required amount of $H_3PO_4$ (85 wt %, Aldrich) was added. The suspension was digested at boiling point (~368 K) until a clear solution was obtained (approximately 5 h). Impregnated precursors were aged at room temperature (overnight), dried at 393 K (12 h) then calcined at 723 K (5 h) under static air atmosphere. For both stages, a slow heating ramp (1 K/min) was tried to avoid mesoporous network collapse [13].

Materials Characterization. Textural properties of mesoporous sieves and impregnated precursors (surface area, $S_g$, pore volume, $V_p$, and pore size distribution, PSD) were determined by $N_2$ physisorption at 77 K (Autosorb-1, Quantachrome) and structural order was analyzed by low-angle (1- 6, $2\theta$ range) X-ray diffraction (XRD, D-5000 Siemens, $Cu_{K\alpha}$ radiation, $\lambda$ = 0.15406 nm).

Wall-thickness for various materials was calculated from the difference between lattice parameter (hexagonal array) and pore diameter [14]:

$$\delta = a_0 - D_{ps} \quad (1)$$

$$a_0 = \frac{2d_{100}}{\sqrt{3}} \quad (2)$$

Where,

$d_{100}$ = Inter-planar distance (from Scherrer´s equation, $d = \lambda/2 \sin(\theta)$, $\lambda$ = X-rays wavelength (Å), $\theta$: diffraction angle

$a_0$ = Cell parameter (hexagonal array), (Å)

$\delta$ = Wall thickness, (Å)

$D_{ps}$ = Pore diameter (from BJH calculations, adsorption data, $N_2$ physisorption isotherm), (Å)

Type, number and strength of surface acid sites were obtained from pyridine thermo-desorption followed by infrared spectroscopy (Fourier Transform Infrared 710 spectrophotometer, Nicolet).

Co content in impregnated samples was quantified by atomic absorption spectroscopy (5000 spectrophotometer, Perkin-Elmer). Chemical analysis (IMP QA201 method) was used to determine Mo concentration. Textural, structural and surface acidity characterizations were also carried out for oxidic impregnated precursors. UV-vis diffuse reflectance spectroscopy (DRS, Cary 5E spectrophotometer, Varian) was applied to study the coordination state of $Co^{2+}$ and $Mo^{6+}$ cations in finely sieved samples (> 80 Tyler mesh, 0.18 mm average particle diameter).

HDS Reaction Test. The impregnated precursor that according to characterization results had the best textural

**Table 1.** Textural and structural characteristics of Al-MCM41 supports prepared

| Sample | Si Source | Al Source | $S_g$[a] ($m^2/g$) | $V_p$[b] ($cm^3/g$) | $d_{100}$[c] (Å) | $a_0$[d] (Å) | $D_{ps}$[e] (Å) | δ[f] (Å) |
|---|---|---|---|---|---|---|---|---|
| SB | $SiO_2$ | AlO(OH) | 1045 | 0.98 | 41.8 | 48.2 | 30.3 | 17.9 |
| SAS | $SiO_2$ | $Al_2(SO_4)_3$ | 998 | 1.07 | 46.2 | 53.3 | 33.8 | 19.5 |
| TSA | TEOS | $Al_2(SO_4)_3$ | 836 | 0.88 | 45.4 | 52.4 | 30.5 | 21.9 |

[a]: Surface area; [b]: Pore volume; [c]: Interplanar distance; [d]: Lattice parameter; [e]: Support pore diameter; [f]: Wall thickness

properties and higher proportion of octahedral $Mo^{6+}$ was treated at 673 K (1 h) under a $H_2S/H_2$ (10 v/v %, Praxair) stream (at 4 L/h) to obtain the final sulfided catalyst. An $Al_2O_3$-supported commercial formulation (IMP DSD14) of similar Co-Mo-P loading prepared also by simultaneous impregnation was used as reference ($S_g$= 227 $m^2/g$, $V_p$= 0.49 $cm^3/g$). HDS activity was studied in a tri-phasic slurry batch reactor (Parr 4562 M). The reaction mixture was prepared by dissolving ~ 0.3 g of DBT in 0.1 L *n*-hexadecane (both from Aldrich) and adding ~0.2 g of sieved catalyst (80-100 Tyler mesh, 0.165 mm average particle diameter). The operating conditions (carefully chosen to avoid external and/or internal diffusional limitations) were $P_{H2}$= 5.59 ± 0.03 MPa, $T_R$= 593 ± 2 K and a 1000 RPM (~105 rad/s) mixing speed. Samples were taken periodically and analyzed in a gas chromatograph Perkin-Elmer AutoSystem XL equipped with flame ionization detector and Econopac-5 capillary column (Alltech). HDS kinetic constants were calculated assuming pseudo-first order behavior regarding DBT concentration (zero order respecting excess $H_2$):

$$k = \frac{-\ln(1-x)}{t} \qquad (3)$$

Where,

*k:* pseudo first order HDS kinetic constant ($s^{-1}$)
*x:* DBT conversion at time *t*
*t:* time (s)
*k* values were normalized by considering reaction volume and mass of catalyst used (*k* expressed in $m^3 kg_{cat.}^{-1}\ s^{-1}$).

## Results and Discussion

Mesoporous Supports. The textural properties of Al-MCM41 supports are shown in Table 1. The materials obtained from silicon oxide showed very similar $S_g$ and pore volume, irrespective of Al source, whereas the ones of the sample prepared from TEOS were lower. In all cases, type IV $N_2$ adsorption isotherms characteristics for mesoporous sieves [15] were found (Fig. 1). Those curves practically did not show hysteresis loop in agreement with that previously reported for Al-MCM41 [16]. The sharp increase in adsorbed volume at 0.3-0.4 relative pressure followed by a plateau indicated capillary

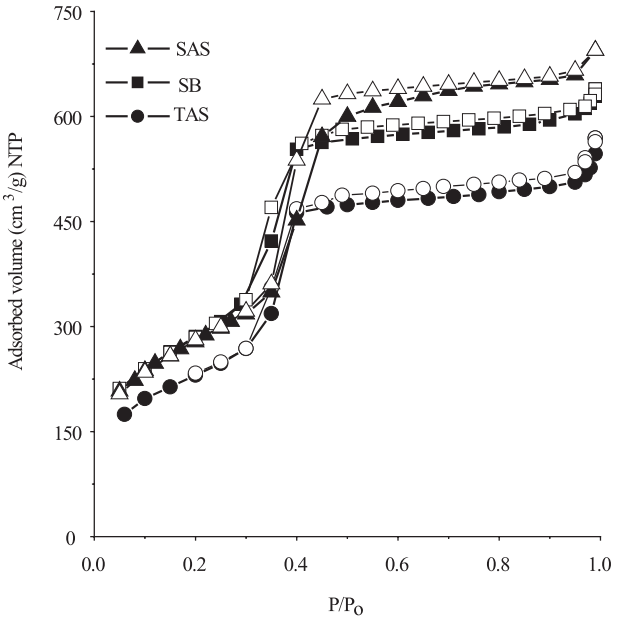


**Fig. 1.** $N_2$ physisorption isotherms (at 77 K) of Al-MCM41 supports prepared. Open symbols: desorption branch.

condensation in mesopores in a narrow diameter range [15], as confirmed by PSD (Barrett, Joyner and Halenda, adsorption branch data), Fig. 2. Although no important differences in PSD for various supports were evident, SAS had pores slightly higher than the rest of oxides.

The (100) low-angle diffraction line produced by hexagonal mesoporous array [17] was observed for all materials although it shifted to lower angles for samples prepared from $Al_2(SO_4)_3$, Fig. 3. The most intense signal found for SB as well as the small (110) [14] signal indicated a more ordered porous network. On the other hand, both samples prepared from aluminum sulfate were less-ordered suggesting higher $Al^{3+}$ incorporation in their walls, as this could be reflected in structural periodicity loss [6]. In this line, TAS was constituted by a rather disordered array.

The wall thickness calculated from equation (1) for various materials are presented in Table 1. According to them, higher amounts of aluminum could be isomorphously incorporated into the walls of TAS and SAS as these would be thickened by $Al^{3+}$ cations intrusion. Our results are close to those obtained from HR-TEM by Landau [5] for Al-MCM41 of

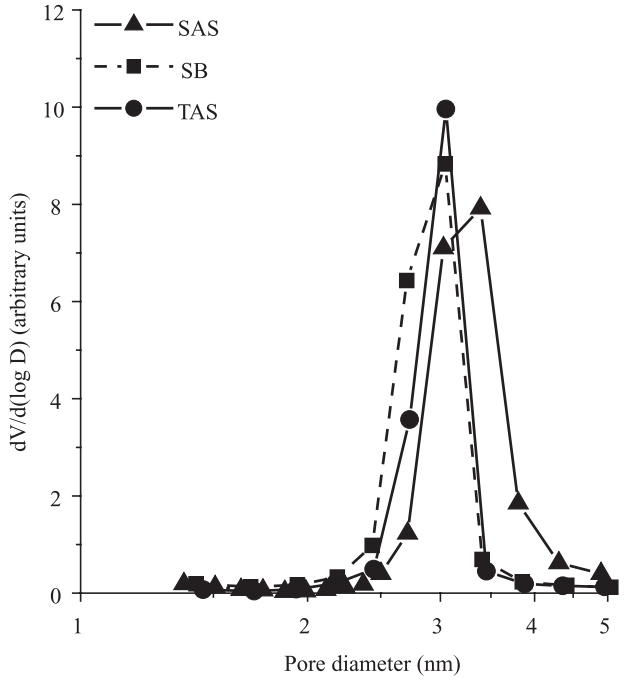


**Fig. 2.** Pore size distributions (from $N_2$ physisorption at 77 K, adsorption branch data) of Al-MCM41 supports prepared.

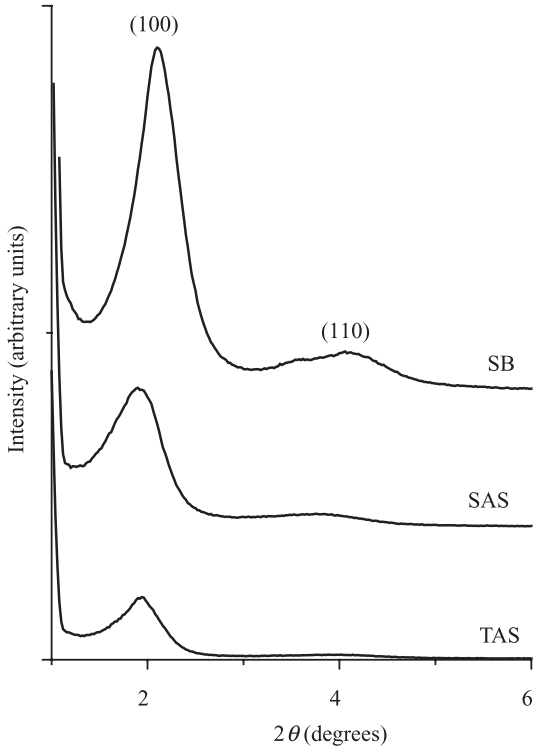


**Fig. 3.** Low-angle X-ray diffractograms of Al-MCM41 supports prepared.

similar composition to our samples (δ~15 Å). It should be taken into account that equation (1) offers an estimate that is influenced by the accuracy of the analytical techniques used (XRD and $N_2$ physisorption) meanwhile by transmission electron microscopy the actual values could be determined.

Strong differences in structural order (Fig. 3) could be a function of the interaction between the Si and Al precursors used. It has been reported that boehmite tends to produce octahedral (extra-framework) $Al^{3+}$ meanwhile aluminum sulfate promotes incorporation of tetrahedral species in $SiO_2$ walls [18], in strong agreement with our findings.

Quantification of surface Brønsted and Lewis acid sites on the mesoporous sieves is shown in Fig. 4 and 5, respectively. The number of medium-strength protonic sites followed the trend TAS > SAS > SB whereas Lewis centers were slightly increased in SB. The tendency found for Brønsted acidity fully agreed with progressively higher $Al^{3+}$ intrusion in MCM41 walls (Table 2), as reported by Mokaya et al. [19]. On the other hand, more segregated $Al^{3+}$ (extra-framework) in SB could be reflected in higher Lewis acidity [11]. From our characterization results, we conclude that compounds that could produce monomeric $Al^{3+}$ species must be preferred as aluminum sources. In this line, Janicke [20] showed that the degree of Al incorporation was strongly influenced by the nature of its source. Accordingly, compounds as aluminum sulfate will produce highly-reactive $Al^{3+}$ cations that could compete with anionic silicate units to coordinate with surfactant molecules and other cationic species present in the reaction mixture. Because of that, they would be likely incorporated in the solid silicate framework. Conversely, colloidal Al

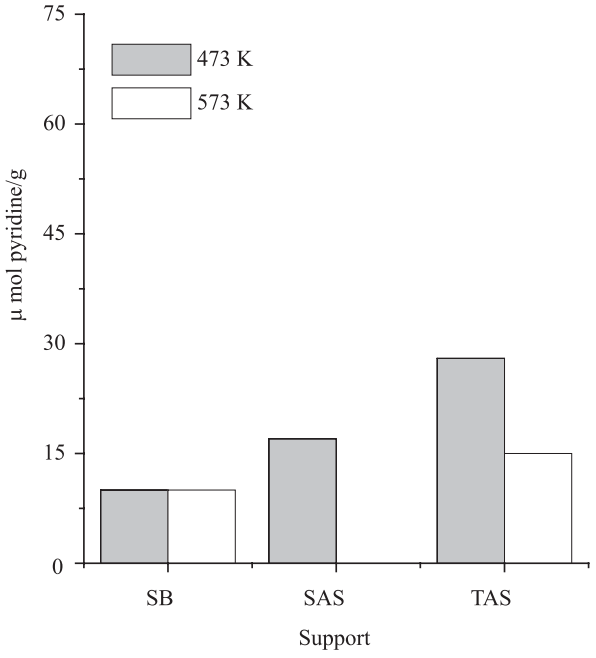


**Fig. 4.** Medium and strong Brønsted acidity (as determined by pyridine thermo-desorption followed by FTIR) of Al-MCM41 supports prepared.

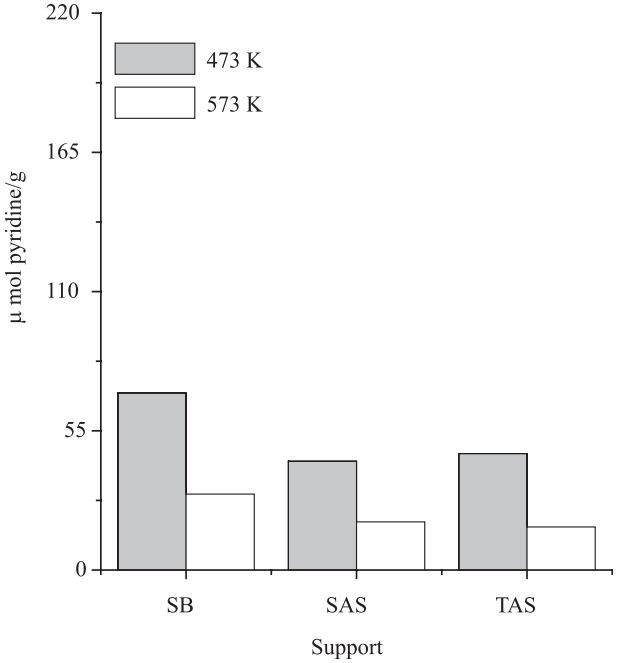


**Fig. 5.** Medium and strong Lewis acidity (as determined by pyridine thermo-desorption followed by FTIR) of Al-MCM41 supports prepared.

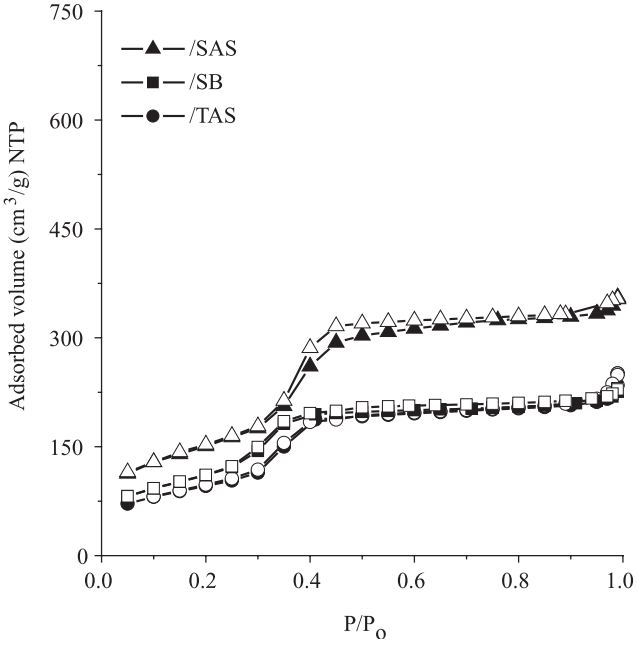


**Fig. 6.** $N_2$ physisorption isotherms (at 77 K) of Co-Mo-P precursors impregnated on the Al-MCM41 supports prepared. Open symbols: desorption branch.

**Table 2.** Experimental and theoretical (considering non-porous phases deposition) textural properties of various CoMoP/Al-MCM41 impregnated precursors prepared

| Sample | $S_g$[a] ($m^2$/g) | $V_p$[a] ($cm^3$/g) | $S_g$* ($m^2$/g) | $V_p$* ($cm^3$/g) |
|---|---|---|---|---|
| CoMoP/SB | 462 | 0.36 | 761 | 0.71 |
| CoMoP/SAS | 548 | 0.55 | 749 | 0.80 |
| CoMoP/TSA | 359 | 0.38 | 615 | 0.65 |

[a]: From $N_2$ physisorption; *: Theoretical values

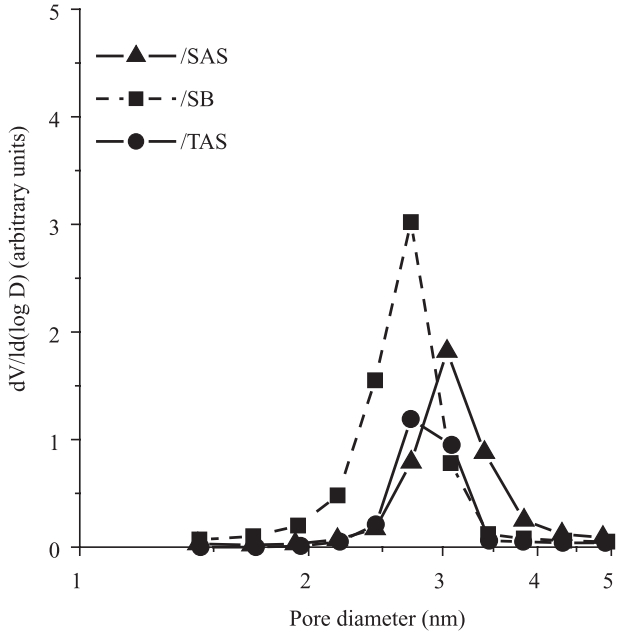


**Fig. 7.** Pore size distributions (from $N_2$ physisorption at 77 K, adsorption branch data) of Co-Mo-P precursors impregnated on the Al-MCM41 supports prepared.

sources (as boehmite with 100% octahedral Al) will tend to form extra-framework six-coordinated species.

Impregnated Precursors. For impregnated precursors, Mo and Co contents were close to target loadings (not shown). In Fig. 6, the $N_2$ adsorption isotherms (77 K) of various Co-Mo-P impregnated precursors can be observed. Although $N_2$ adsorbed volumes strongly decreased, as to that of the corresponding supports, all impregnated materials appeared to conserve the original Al-MCM41 mesoporous array. This was especially true for the SAS-supported material. Following the trend observed for the corresponding Al-MCM41 supports, the average pore diameter of this sample was slightly higher as to those of the rest of impregnated solids, Fig. 7. The textural properties of all impregnated samples are presented in Table 3. $S_g$* and $V_p$* represent the theoretical surface area and pore volume values assuming that texture losses were related just to incorporation of non-porous oxidic impregnated phases ( CoO, $MoO_3$ and $PO_4^{3-}$). It is clear that CoMoP/SAS was the material that retained the best texture. In order to assess the homogeneity of supported oxidic molybdenum distribution on various impregnated precursors, the model proposed by Landau [5] (cylindrical pores) was applied, namely:

$$D_p^* = \sqrt{\left(1 - \frac{y_{MoO_3} / \rho_{MoO_3}}{V_p(1 - y_{MoO_3})}\right) D_{ps}^{\,2}} \qquad (4)$$

Where,

$D_p^*$ = Impregnated precursor pore diameter, (Å)
$y_{MoO3}$ = $MoO_3$ mass fraction in impregnated precursor
$\tilde{n}_{MoO3}$ = $MoO_3$ density (3.6 g/cm$^3$)
$V_p$ = Support pore volume, (cm$^3$/g)*
$D_{ps}$ = Support pore diameter, (Å)*
* (from BJH calculations, adsorption data, $N_2$ physisorption isotherm)

The calculated average pore diameter values were compared with the experimental ones, Table 3. Although no important differences among them were observed, all the actual $D_p$ values were lower than the calculated ones suggesting uneven Mo distribution. This fact confirmed that textural losses were owing to partial pore plugging.

From low-angle X-ray diffractograms of impregnated precursors (not shown), the (100) line related to hexagonal mesoporous array was not evident in any case. This indicated that although $N_2$ adsorption isotherms shape suggested preservation of the mesoporous network at some extent, the structural order was lost because supported phases were not very homogeneously distributed.

All the impregnated precursors had much higher acidity than the corresponding supports, Fig. 8 and 9. This effect was more pronounced for CoMoP/TAS that showed the highest amount of both protonic and Lewis sites. The acidity increase could be mainly related to deposited $PO_4^{3-}$ groups [21]. There seemed to be a relationship between initial amount of protonic sites on supports and increase of acidity in impregnated precursors. This could be rationalized by taking into account that during impregnation phosphate species (from $H_3PO_4$) are prone to react with surface OH´s [21]. Thus, more dispersed phosphate species responsible for increased surface acidity could be expected on TSA, as indeed was found. Based on our results, phosphorous addition strongly augments acidity of MCM41 surface providing an effective simpler alternative method to the traditional strategy of incorporating $Al^{3+}$ cations in high to moderate concentration [6, 16]. In addition, increas-

**Table 3.** Comparison between experimental and calculated average pore size of CoMoP/Al-MCM41 impregnated precursors

| Sample | $D_p$[a] (Å) | $D_p$*[b] (Å) | Difference (Å) |
|---|---|---|---|
| CoMoP/SB | 27.2 | 29.2 | 2.0 |
| CoMoP/SAS | 30.5 | 32.8 | 2.3 |
| CoMoP/TSA | 27.2 | 29.3 | 2.1 |

[a]: From $N_2$ adsorption data; [b]: Calculated from equation (4), see text.

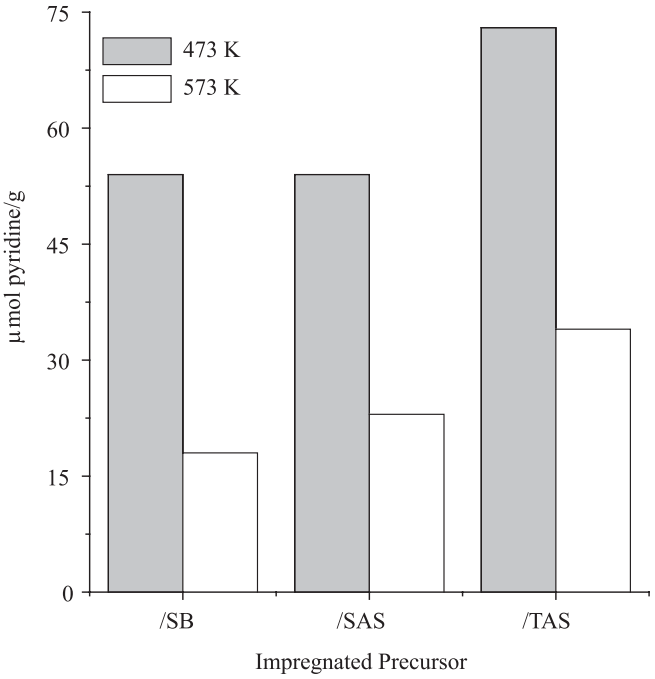


**Fig. 8.** Medium and strong Brønsted acidity (as determined by pyridine thermo-desorption followed by FTIR) of Co-Mo-P precursors impregnated on Al-MCM41 supports prepared.

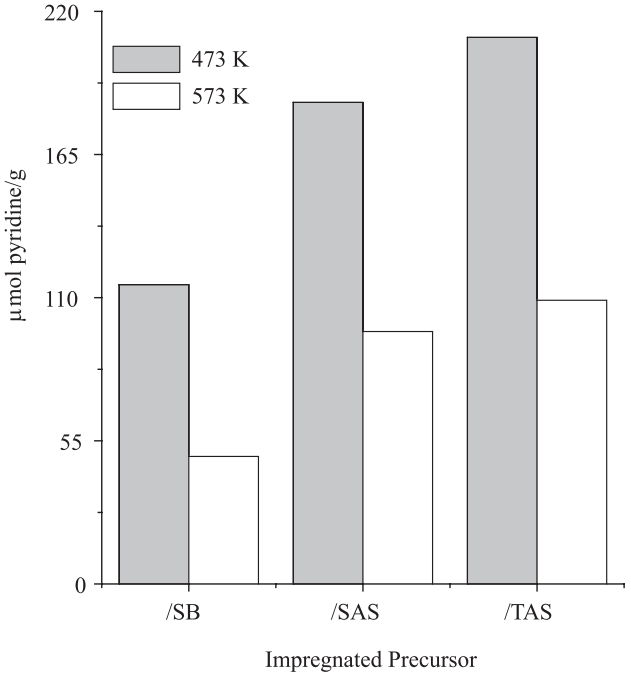


**Fig. 9.** Medium and strong Lewis acidity (as determined by pyridine thermo-desorption followed by FTIR) of Co-Mo-P precursors impregnated on Al-MCM41 supports prepared.

ing surface acidity by this method allows to overcome structural collapse that occur when high-Al mesoporous sieves are simultaneously impregnated with Co-Mo-P solution which is strongly acidic (1.8 < pH < 2) [22]. To test the susceptibility of Al-MCM41 to $Al^{3+}$ leaching under acidic impregnation conditions, one solid of $SiO_2/Al_2O_3$=50 prepared through SAS method was contacted with the corresponding Co-Mo-P solution by incipient wetness method. As a result, the material lost about 80 % of its original surface area, very probably due to structural collapse by $Al^{3+}$ extraction from the solid matrix.

In Fig.10 UV DRS spectra of calcined impregnated precursors can be observed. A wide band attributed to octahedral and tetrahedral $Mo^{6+}$ (230-330 and 250-280 nm, respectively) [23] was observed for all samples. The blue-shifted bands observed for solids supported on SB and TAS could be originated in higher proportion of anions in tetrahedral coordination (*i.e.*, $MoO_4^{2-}$) of lower number of next-nearest neighbours, *i.e.*, of higher dispersion [24]. On the opposite, the shift to lower energies of the absorption edge of CoMoP/SAS suggested increased amount of octahedral $Mo^{6+}$. These species have been claimed to be more easily reducible than molybdenum anions in tetrahedral coordination [6]. Then, TAS and SB seemed to promote stronger interaction with supported oxidic Mo probably because of their higher number of strong acid sites (Fig. 4 and 5). The signal registered in the visible region (at 500-700 nm, Fig. 11) was related to tetrahedral $Co^{2+}$ [23]. No differences were observed among these signals for various oxidic impregnated precursors.

DBT HDS Reaction Test. The sample that according to our characterization data had the best textural properties and the highest proportion of more reducible octahedral $Mo^{6+}$ was CoMoP/SAS. Then, this would be our best candidate to provide an effective HDS catalysts. A comparison between the DBT HDS kinetic constant (pseudo first order) of the corresponding sulfided catalyst and that of an $Al_2O_3$-supported commercial formulation is shown in Fig. 12. The solid supported in mesoporous sieve promoted ~30% higher HDS activity. It is worth mentioning that the result found is superior to that previously reported in the literature. Indeed, CoMo/Al-

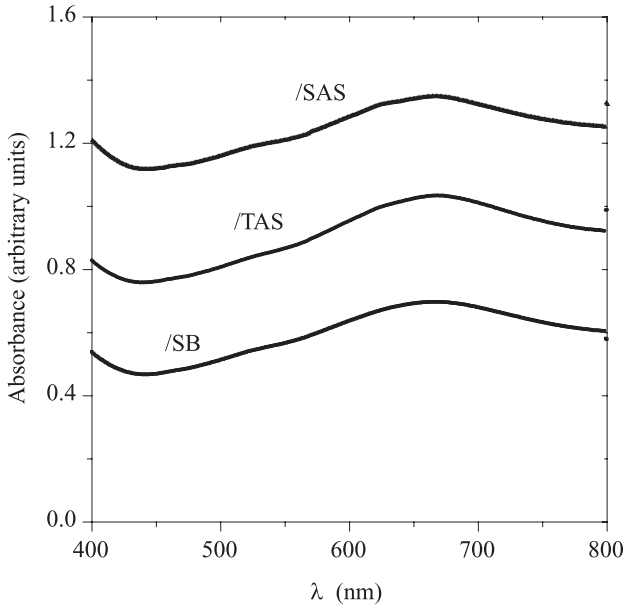


**Fig. 11.** Visible region DRS spectra of Co-Mo-P precursors impregnated on Al-MCM41 supports prepared.

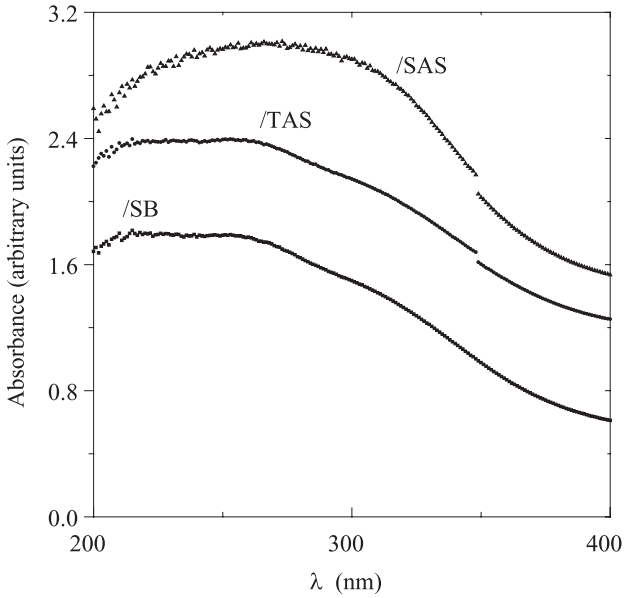


**Fig. 10.**- UV DRS spectra of Co-Mo-P precursors impregnated on Al-MCM41 supports prepared.

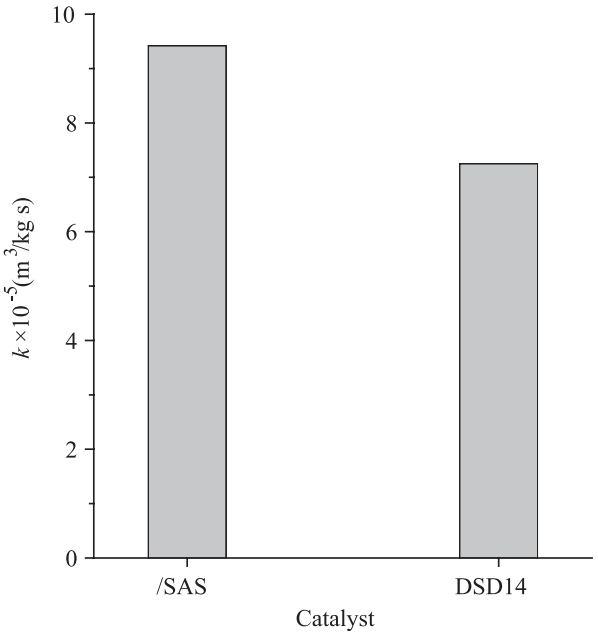


**Fig. 12.** Pseudo first order DBT HDS kinetic constants promoted by catalysts studied. $P_{H2}$= 5.59 ± 0.03 MPa, $T_R$= 593 ± 2 K, 1000 RPM mixing speed, solvent: *n*-hexadecane.

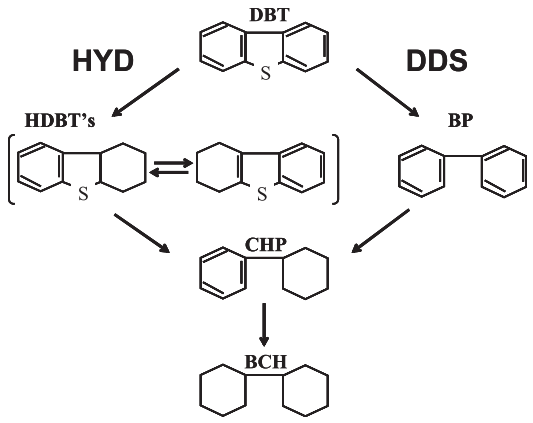


**Fig. 13.** DBT HDS reaction network over sulfided $CoMo/Al_2O_3$ (from [26]).

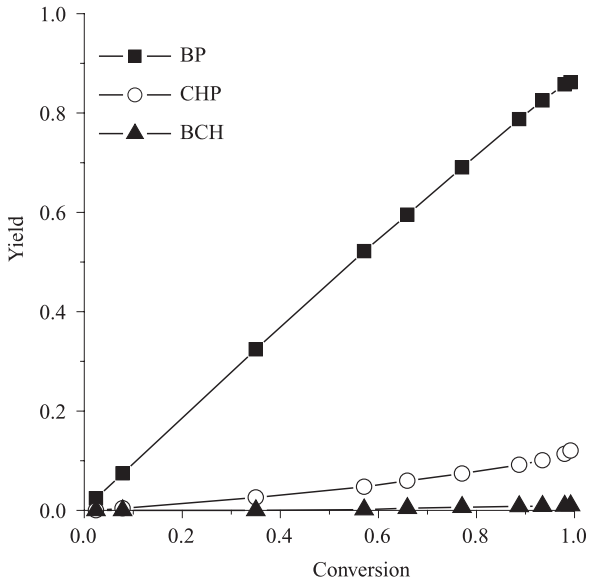


**Fig. 14.** Yield vs. Conversion plot (DBT HDS) of sulfided CoMoP/SAS catalyst sulfided at 673 K. Reaction conditions specified in Fig. 12 caption.

MCM41 catalyst of composition alike to that of our samples had shown similar or lower performance, as to that of $Al_2O_3$-supported commercial formulations, in the hydrotreatment of middle distillates [10, 25]. Our results strongly suggested that sulfided phases were better dispersed when impregnated on SAS mesoporous sieve. We believe that P incorporation could be playing a decisive role on the observed behavior. By increasing Lewis surface acidity (Fig. 9), the good textural properties (Table 1) of that otherwise low-acidity Al-MCM41 support (Fig. 5), could be exploited to efficiently disperse Mo sulfide.

Fig. 13 shows the DBT HDS reaction routes proposed by Houalla [26] meanwhile in Fig. 14 selectivity to various products over sulfided CoMoP/SAS is presented. In agreement to that previously reported [27] for catalyst of similar Co/Mo ratio supported on siliceous MCM41, direct desulfurization (DDS) to biphenyl (Fig. 13) was favored over CoMoP/SAS, the pattern being very similar to that registered for the $Al_2O_3$-supported solid. This fact suggested good Mo promotion by Co [28, 29]. Some authors have found cracking products from DBT HDS, even in the case of CoMo catalysts supported in non-doped siliceous MCM-41 [27]. In our case, no cracking products were observed (toluene, benzene, etc.) which meant that increased protonic acidity produced by phosphorous addition was not strong enough to promote those reactions under the conditions studied.

## Conclusions

Al-MCM-41 ($SiO_2/Al_2O_3$ = 200) from various Al and Si sources were synthesized and used as Co-Mo-P catalysts support. Improved textural properties were registered for the samples where $SiO_2$ was used as Si source. $Al(SO_4)_3$ produced solids of better $Al^{3+}$ integration in the tetrahedral walls of MCM41. Surface acidity was notably increased after calcining impregnated Co-Mo-P probably due to $PO_4^{3-}$ groups deposition. After sulfiding ($H_2S/H_2$, 673 K), the precursor of both the best texture and the highest proportion of octahedral $Mo^{6+}$ (the one supported on Al-MCM41 from $SiO_2$-$Al(SO_4)_3$) was ~30% more active in dibenzothiophene hydrodesulfurization than an $Al_2O_3$-supported commercial formulation of similar Co-Mo-P loading. The high HDS activity and predominant selectivity to biphenyl suggested good Mo promotion by Co in that Al-MCM41-supported catalyst.

## Acknowledgements

The authors recognize financial support from Instituto Mexicano del Petróleo (D.1020 grant), Universidad Autónoma Metropolitana and CONACyT. One of us (A. Hernández) also acknowledges the thesis grants received (IMP 87192 and UJAT 017UJAT-T.T./03).

## References

1. Xu, X.; Waller, P.; Crezee, E.; Shan, Z.; Kapteijn, F.; Moulijn, J.A., in: Scientific Bases for the Preparation of Heterogeneous Catalysts, Gaigneaux, E.; De Vos, D.E.; Grange, P.; Jacobs, P.A.; Martens, J.A.; Ruiz, P.; Poncelet, G. Eds. *Stud. Surf. Sci. Cat.* Vol. 143, Elsevier, The Netherlands, **2002**, 1019-1026.
2. Flego, C.; Arrigoni, V.; Ferrari, M.; Riva, R.; Zanibelli, L. *Cat. Today* **2001**, *65*, 265-270.
3. Breysse, M.; Afanasiev, P.; Geantet, Ch.; Vrinat, M. *Cat. Today* **2003**, *86*, 5-16.
4. Kooyman, P.J.; Waller, P.; van Langeveld, A.D.; Song, C.; Reddy, K.M.; Van Veen, J.A.R. *Catal. Lett.* **2003**, *90*, 131-135.
5. Landau, M.V.; Vradman, L.; Herskowitz, M.; Koltypin, Y.; Gedanken, A. *J. Catal*. **2001**, *201*, 22-36.

6. Klimova, T.; Calderón, M.; Ramírez, J. *Appl. Catal.* A **2003**, *240*, 29-40.
7. Ramírez, J.; Ruiz, L.; Cedeño, L.; Harlé, V.; Vrinat, M.; Breysse, M. *Appl. Catal.* **1993**, *93*, 163-180.
8. Isoda, T.; Takase, Y.; Kusakabe, K.; Morooka, S. *Energy&Fuels* **2000**, *14*, 585-590.
9. Cheng, M.; Kumata, F.; Saito, T.; Komatsu, T.; Yashima, T. *Appl. Catal.* A **1999**, *183*, 199-208.
10. Song, Ch.; Reddy, K.M. *Appl. Catal.* A **1999**, *176*, 1-10.
11. Corma, A.; Martínez, A.; Martínez-Soria, V.; Montón, J.B. *J. Catal*. **1995**, *153*, 25-31.
12. Reddy, K.M.; Wei, B.; Song, Ch. *Cat. Today* **1998**, *43*, 261-272.
13. Lensveld, D.J.; Mesu, J.G.; van Dillen, A.J.; de Jong, K.P. *Micropor. Mesopor. Mater*. **2001**, *44-45*, 401-407.
14. Ciesla, U.; Schüth, F. *Micropor. Mesopor. Mater*. **1999**, *27*, 131-149.
15. Wang, A.; Wang, Y.; Kabe, T.; Chen, Y.; Ishihara, A.; Qian, W.; Yao, P. *J. Catal*. **2002**, *210*, 319-327.
16. Biz, S.; Occelli, M.L. *Catal. Rev.–Sci. Eng*. **1998**, *40*, 329-407.
17. Turaga, U.; Song, Ch. *Cat. Today* **2003**, *86*, 129-140.
18. Corma, A. *Chem. Rev*. **1997**, *97*, 2373-2419.
19. Mokaya, R.; Zones, W.; Luan, Z.; Alba, M.D.; Klinowski, J. *Catal. Lett*. **1996**, 37, 113.
20. Janicke, M.; Kumar, D.; Stucky, G.D.; Chmelka, B.F. *Stud. Surf. Sci. Cat*. Vol. 84, Elsevier, The Netherlands, **1994**, 243-250.
21. Sun, M.; Nicosia, D.; Prins, R. *Cat. Today* **2003**, 86, 173-189.
22. Marín, C.; Escobar, J.; Galván, E.; Murrieta, F.; Zárate, R.; Vaca, H. *Fuel Proc. Tech*. **2004**, in press.
23. Ramírez, J.; Contreras, R.; Castillo, P.; Klimova, T.; Zárate, R.; Luna, R. *Appl. Catal.* A **2000**, *197*, 69-78.
24. Weber, R.S. *J. Catal.* **1995**, *151*, 470-474.
25. Turaga, U., Song, Ch. *Prepr. Pap.-Am. Chem. Soc., Div. Pet. Chem*. **2001**, *46*, 275-279.
26. Houalla, M.; Nag, N.K.; Sapre, A.V.; Broderick, D.H.; Gates, B.C. *AIChEJ* **1978**, *24*, 1015-1021.
27. Wang, A.; Wang, Y.; Kabe, T.; Chen, Y.; Ishihara, A.; Qian, W. *J. Catal*. **2001**, *199*, 19-29.
28. Bataille, F. ; Lemberton, J.L.; Pérot, G.; Leyrit, P.; Cseri, T:, Marchal, N.; Kasztelan, S. *Appl. Catal.* A **2001**, *220*, 191-205.
29. Mijoin, J.; Pérot, G.; Bataille, F.; Lemberton, J.L.; Breysse, M.; Kasztelan, S. *Catal. Lett*. **2001**, *71*, 139-145.